Journal of Techniques, ISSN: 2708-8383, Vol. 6, No. 4, 2024, Pages 40-47
DOI: https://doi.org/10.51173/jt.v6i4.1743

JOURNAL OF TECHNIQUES

Journal homepage: http://journal.mtu.edu.iq

RESEARCH ARTICLE - ENGINEERING (MISCELLANEOUS)

Miniaturized Inset-Fed Microstrip Patch Sensor Based on Meander-Line Slot for Water Measurement Applications

Aya Khalid Hadi[1*], Mahmood Farhan Mosleh[1], Raed A. Abd-Alhameed[2]

[1]Electrical Engineering Technical College, Middle Technical University, Baghdad, Iraq

[2]Faculty of Engineering and Informatics, University of Bradford, Bradford, United Kingdom

[*] Corresponding author E-mail: aya.khalid.hadi.1999@gmail.com

Article Info.

Article history:

Received
09 July 2023

Accepted
22 September 2023

Publishing
31 December 2024

Abstract

This article introduces a high-sensitive microstrip-patch sensor-based meander-line slot structure for water measurement applications. The HFSS software tool is employed to design and simulate the proposed system. The inset-fed sensor size is 60×50×1 mm3 and is printed on a low-cost FR-4 dielectric substrate. The meander-line slots resonator is used in the proposed design to produce strong and concentrated electric fields while increasing the energy output by focusing the current in a narrow area. In addition to enhancing sensitivity, it decreases the sensor dimension, provides a region with strong electric fields, and increases the interaction area with the water. This sample needs to be tested. For the unloaded condition, the miniaturized sensor is resonant at 2.863 GHz with a reflection coefficient (S11) amplitude equal to -30.219 dB. At the same time, the miniaturized sensor is deep at 2.144 GHz, 2.148 GHz, and 3.14 GHz for DI-water, freshwater, and seawater-loaded conditions. According to simulated results, high sensitivity values are found. The sensor has sensitivities of 3.14 and 1.21 for DI water and seawater, respectively. The high sensitivity values of the proposed sensor indicate that any slight change in the εr around the sensing area of the proposed sensor will be translated into significant changes in the resonant frequency and the recorded output results.

Publisher: Middle Technical University

Keywords: Inset-Fed Microstrip-Patch Sensor; Meander-Line Slot; Sensitivity; Water Measurement.

1. Introduction

The various microwave sensors' detecting capabilities, which rely primarily on the resonance principle, are gaining growing interest for use in bio-sensing, microfluidic, environmental monitoring, and industrial applications due to their low cost, small size, compatibility with wireless electronics, and the progressing fabrication technologies like additive manufacturing [1-2]. However, when a lossy object, such as a dielectric or conductor, is placed in the antennas near the field, the printed antenna's performance can degrade [3]. As a result, changes in the frequency resonance (f_r), polarization, reflection coefficients (S_{11}), and radiation distortions may occur [4]. Because of the material's dielectric properties, antenna performance can occasionally be fine-tuned to meet a given criterion. Microwave sensor-antennas have become more attractive in liquid characterization applications than conventional techniques due to their capabilities and advantages. Moreover, the sensor-antenna structures are found to be more efficient and straightforward, avoiding the use of markers such as fluorescent molecules and magnetic or gold particles. Such techniques can provide high accuracy, low processing time, inexpensive, and need a few microliters of samples for characterization [5]. The patch antenna structure is a radio antenna characterized by a conductive patch mounted on a dielectric substrate layer with a ground plane [6]. Due to their low profile, simple construction, and ability to work with both planar and non-planar circuits, patch antennas have received significant attention in recent years. Microstrip patch antennas come in many different forms and sizes, most used as rectangular, square, and circular. Rectangular patches with radiation properties and simple fabrication are the most common. The patch antenna quickly gained popularity and is now used for satellite and mobile communication, GPS, Wi-Fi, radar, rectenna, telemedicine, and other applications [7]. Munson and Howell implemented the first truly functional design at the start of the 1970s [8-11].

This article presents a low-cost, high-sensitivity patch sensor using a meandering-line slot. The miniaturized sensor is introduced for water measurement identification. The FR-4 dielectric substrate of 60×50×1 mm^3 size is picked up in the design. The meander-line slots resonator technique is employed. The proposed sensor shows a current concentrated in a narrow area compared to another. By current concentration, an amount of energy will be produced there with high sensitivity achieved. The specific design aims to reduce the sensor dimensions, enhance sensitivity, provide a region with strong electric fields, and increase the interaction area with the water sample to be tested. The miniaturized sensor's simulated results showed that the sensor is resonant at 2.863 GHz for the unloaded condition. At the same time, it is resonant at 2.144 GHz for DI-Water, 2.148 GHz for Freshwater, and 3.14 GHz for seawater. The HFSS tool designs and simulates the proposed sensor [12].

Nomenclature & Symbols			
DI-Water	Distilled-Water	HFSS	High Frequency Structure Simulator
h	Substrate Height	L	Substrate Length
W	Substrate Width	L_p	Patch Length
W_p	Patch Width	α	Attenuation Coefficient
Np/m	Neper Per Meter	S/m	Siemens Per Meter
L_{fe}	Edge-Feedline Length	W_{fe}	Edge-Feedline Width
L_g	Inset Gap	W_g	Inset Distance
L_f	Feedline Length	W_f	Feedline Width
tan δ	Loss Tangent		

2. Sensor Design Methodology

The proposed inset-fed Microstrip sensor structure is shown in Fig. 1. The low-priced FR4-epoxy dielectric material of ε_r =4.4 and tan δ = 0.02 is a substrate in the proposed sensor design. The total sensor size is 60×50×1 mm^3. The patch with a rectangular shape is mounted on the substrate with a full scope of 14.68×18.75 mm^2. The 50Ω inset-fed feedline is used to feed the proposed sensor. An entire ground plane is applied on the other substrate's face. The different geometrical details of the proposed sensor are shown in Table 1. The meander-line slots resonator is employed in the proposed design to concentrate the current in a narrow area and increase the amount of energy produced there compared to other areas, and high sensitivity will be recorded. The specific design is intended to decrease the sensor dimension, enhance sensitivity, give a region with good electric fields, and increase the interaction area with the water sample that is to be tested.

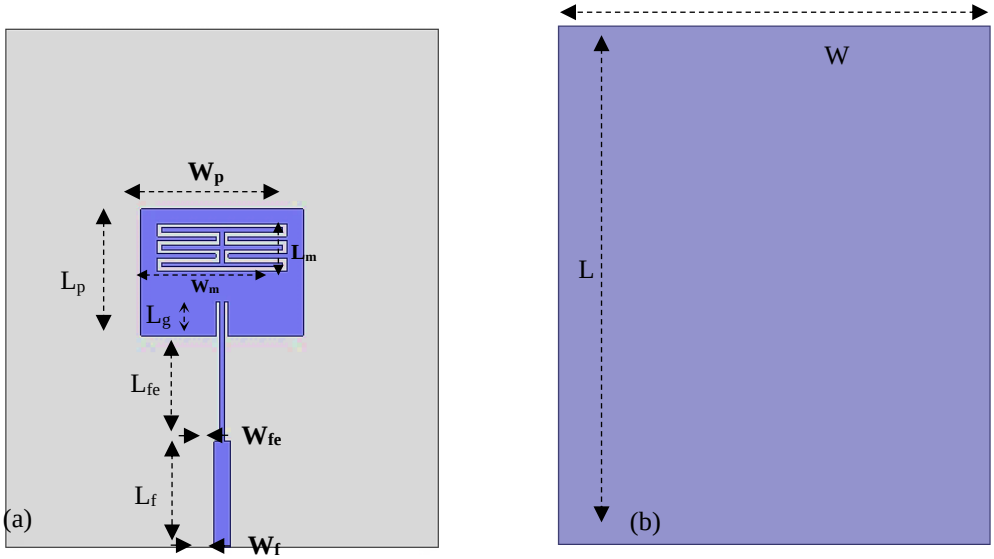

Fig. 1. Proposed Sensor structure; (a) Top View, and (b) Back View

Table 1. Geometrical details of the proposed sensor structure

Parameters	L	W	L_p	W_p	L_m	W_m	h
Value (mm)	60	50	14.68	18.75	5.5	15	1
Parameters	L_{fe}	W_{fe}	L_g	W_g	W_f	L_f	L_s
Value (mm)	12.25	0.45	3.919	0.478	1.911	12.25	0.5

In Fig. 2, the design methodology steps of the proposed sensor are presented. In Fig. 2(a), a conventional inset-fed microstrip patch sensor is introduced. Equations 1 and 2 are used to build and design the traditional structure [13]. The patch with a rectangular shape is printed on an FR4 dielectric substrate with a size equal to 29.375×37.5 mm^2. A fully ground plane is applied and printed on the bottom substrate face. The one-topped inset-fed microstrip line with 50 Ω input impedance feeds the antenna. The calculated feedline width and length are 1.911 mm and 12.25 mm. The edge-feedline width and length are 0.452 mm and 6.75 mm, respectively. Finally, the inset gap equals 0.478 mm, and the inset distance is 4.7 mm.

$$\varepsilon_{eff} = \frac{\varepsilon_r+1}{2} + \frac{\varepsilon_r-1}{2}\left[\frac{1}{\sqrt{1+12\left(\frac{h}{w}\right)}}\right] \quad (1)$$

$$W = \frac{C}{2f_o\sqrt{\frac{\varepsilon_r+1}{2}}} \quad (2)$$

Where: C is speed of light, ε_r is relative permittivity, εeff is the effective dielectric constant, and is the microstrip feedline width.

A slit-line technique is used and applied in the conventional sensor structure to introduce a parasitic capacitance in the antenna to reduce the size and shift the antenna operating frequency, as seen in Fig. 2(b). The slit-line dimensions are 1×30 mm^2, etched out from the patch.

Next, a single meander-line slot structure is inserted, as seen in Fig. 2(c). Moreover, double meander-line slot structures are presented in Fig. 2 (d). The single and double meander-line slot technique is applied to miniaturize the sensor and achieve a lower resonance frequency due to an increase in the current path that flows in the patch more than the straight line. A miniaturized patch sensor is introduced in Fig. 2(e). The meander-line slots resonator concentrates the current in a narrow location and dramatically increases the amount of energy produced there compared to other areas. Any liquid dropped in this region will affect the field lines and alter the recorded response from the sensor. A drop of water is placed in the meander-line slots area due to the highest electric field to measure a water sample with high sensitivity documented.

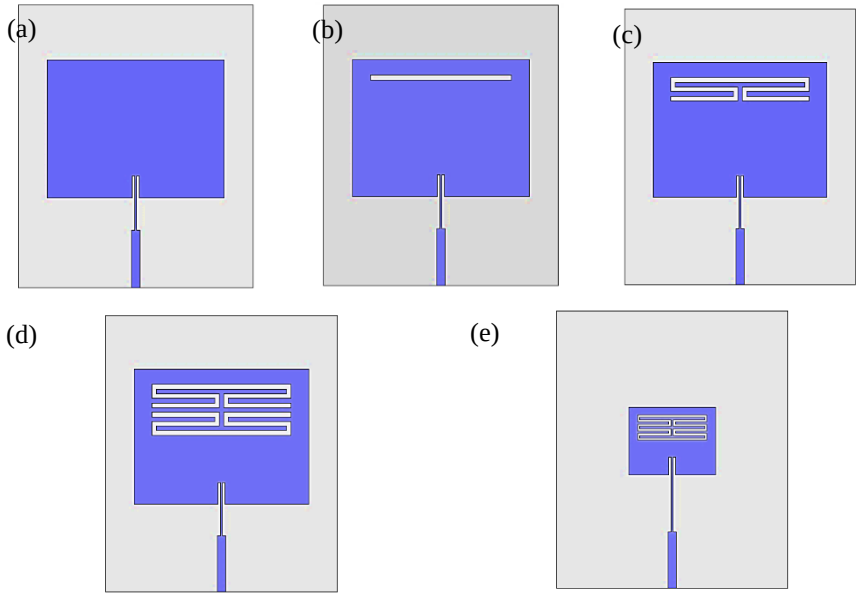

Fig. 2. Design methodology of the proposed patch sensor; a) Conventional structure, b) Conventional design based on slit-line structure, (c) Sensor-based single meander-line slot structure, (d) Sensor-design based double meander-line slot structures, and (e) Miniaturized microstrip patch sensor

In Fig. 3, the unloaded design is simulated, and the corresponding S_{11} is evaluated for all design steps: conventional design, conventional design with slit-line, sensor design with single and double meander slot structure, and miniaturized microstrip patch sensor. The S_{11} of the traditional patch sensor is presented. The conventional design system shows a resonance frequency at 2.3 GHz with a value equal to -13.3dB ranging from 2.31 GHz to 2.34 GHz. A traditional sensor-based slit-line system is simulated, and S_{11} is evaluated. The method-based slit-line showed a resonance frequency at 1.95 GHz with a size reduction of about 15.21% compared with the conventional design. Moreover, another resonance frequency at 4.45 GHz is generated. The first resonance ranges from 1.94 GHz to 1.96 GHz, while the second resonance ranges from 4.43 to 4.47 GHz.

Next, the S_{11} of the microstrip patch sensor with a single meander-line slot is simulated and evaluated. The proposed design-based meander slot is resonance at 1.5 GHz. Moreover, other resonance frequencies are generated at 1.93 GHz, 3.7 GHz, and 4.45 GHz, respectively. This technique showed a size reduction of about 34.78% compared with the conventional design. A microstrip sensor-based double meander slot structure is simulated, and the S_{11} is presented in Fig. 3. The design is found to resonate at 1.04 GHz.

Moreover, a second resonance frequency is observed at 1.93 GHz. According to the evaluated results, this technique presented a size reduction of about 54.79% compared with the conventional design. The corresponding S_{11} of the miniaturized microstrip sensor structure is found and illustrated in Fig. 3. The miniaturized form showed a resonance frequency of 2.86 GHz with a bandwidth of 40 MHz (2.84 - 2.88 GHz).

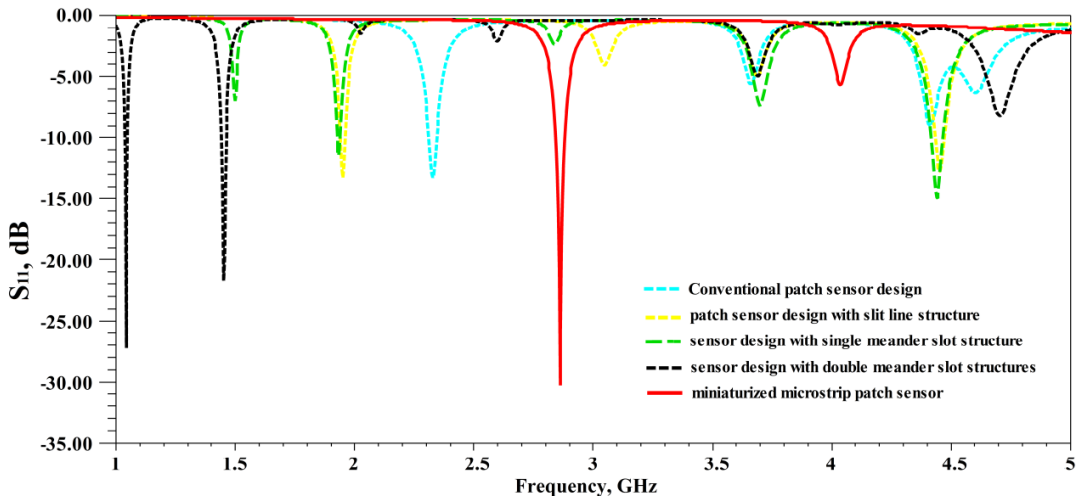

Fig. 3. S_{11} spectra of the evolution steps of the unloaded microstrip patch sensor design

The electrical field behaviors of a conventional-sensor design, a conventional design-based slit-line structure, a sensor with a single meander slot structure, a sensor with double meander slot structures, and a miniaturized microstrip patch sensor are presented in Fig. 4. The electric current is concentrated at the patch's center area, left and right edges in a conventional sensor, as seen in Fig. 5(a). When the slit line is inserted and etches out from the patch surface, the electric current is concentrated at the lower patch area at the edges, as seen in Fig. 5(b). Finally, the electric current paths in the sensor-based meander-line slot structure are evaluated, as seen in Fig. 5(c, d, and e). It is noticed that the current is strongly concentrated around/inside the meander-line slot structure with a lower current concentration at another patch area. The meander-line slots resonator technique concentrates the field in a small area, and the e-field strength will be greater than in other areas. Any liquids dropped in this area will lead to changes, distort the field lines, and alter the recorded sensor response.

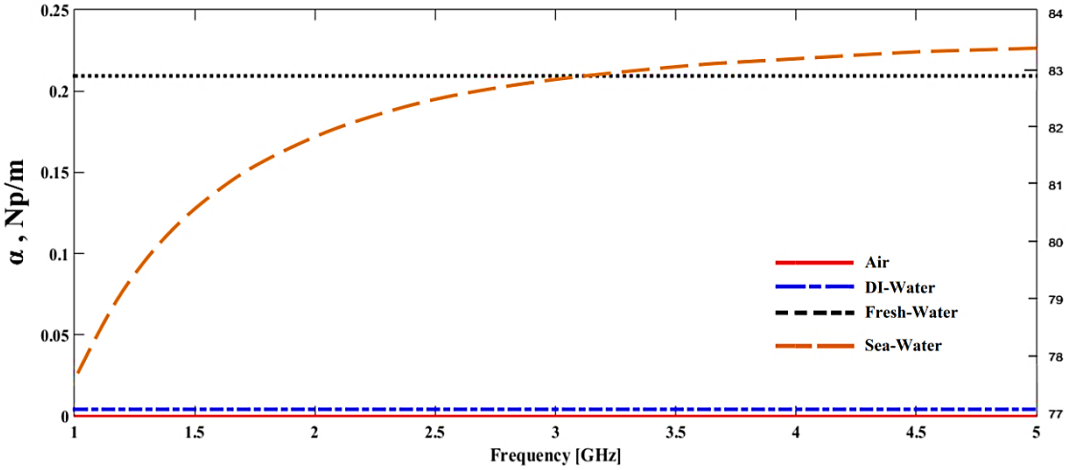

Fig. 4. Attenuation-coefficient spectra of air and different water types

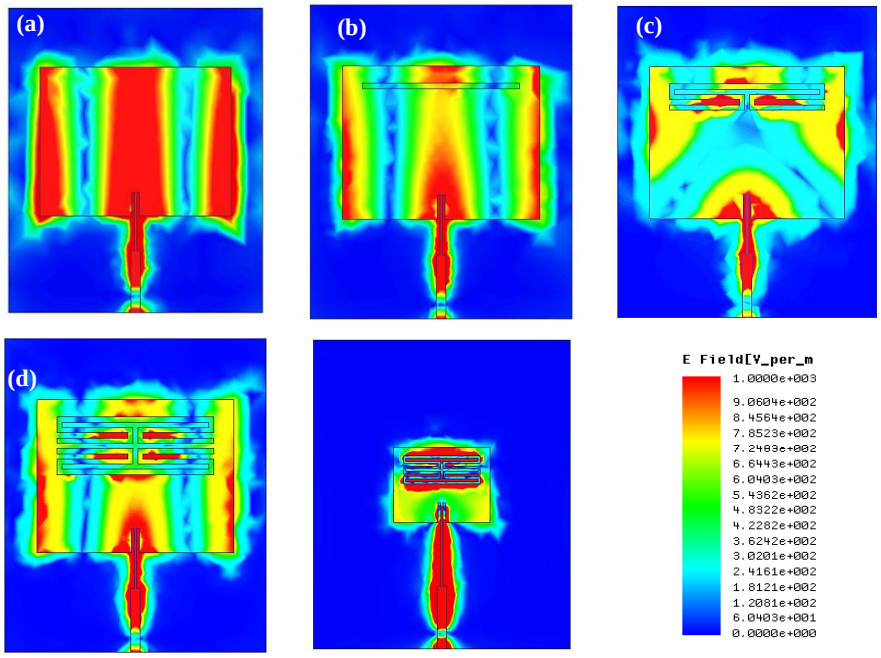

Fig. 5. Electric fields behavior of the proposed sensor design; a) Conventional design, b) Conventional design with slit-line structure, (c) Sensor design with single meander slot structure, (d) Sensor design with double meander slot structures, and (e) Miniaturized microstrip patch sensor

3. Sensitivity Theory and Comparison

3.1. Theoretical background

The water properties differ from air, which is characterized by high permittivity (ε) and electrical conductivity (σ). According to these properties, the electromagnetic behavior through water differs from that of air. The relative permittivity of the water, seawater, freshwater, and distilled water equals 81. However, each type of water has a different conductivity value; seawater conductivity is four s/m, freshwater is 0.01 s/m, and distilled water is 0.0002 s/m. Using Eq. 3 [13], the attenuation coefficients of all types are found, as shown in Figure 4. According to the evaluated result, the seawater has the highest attenuation and increases rapidly with the frequency.

$$\alpha = \omega \sqrt{\frac{\mu\varepsilon}{2}\left[\sqrt{1+\left[\frac{\sigma}{\omega\varepsilon}\right]^2}-1\right]} \quad \text{Np/m} \tag{3}$$

Where ε is permittivity, μ is permeability, ω is angular frequency, and σ is conductivity.

To measure and identify the water type, a drop of water will be dropped on the patch, as seen in Fig. 6. When the electrical current flows in the patch-based meander-line slot, E-field lines are generated between adjacent strip lines due to the coupling phenomenon. The generated fields will be crossed through the water drop. Due to the properties of each water type in terms of different conductivity and attenuation values, another behavior will be achieved when the field is passed through. As a result, another S_{11} will be recorded.

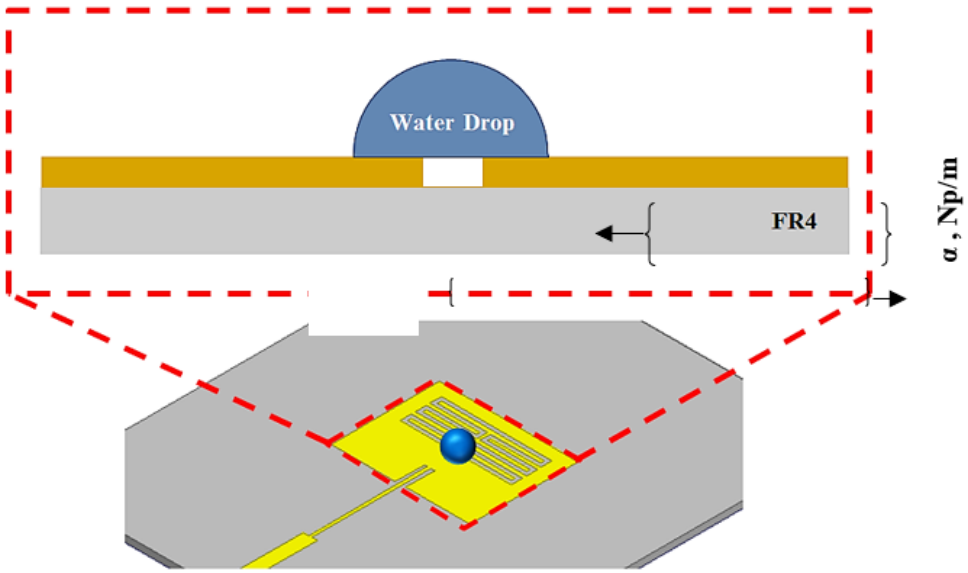

Fig. 6. Testing procedure

3.2. Sensitivity results and comparison

Drops of different water types are loaded on the proposed microstrip sensor and tested. The first resonant frequency of each class is evaluated, and the shift in the frequency is measured and compared with the unloaded case, as seen in Fig. 7.

Firstly, the S_{11} is found for the unloaded case. The evaluated result showed a single resonance frequency at 2.68 GHz with an S_{11} value equal to -30.219 dB.

Then, a drop of distilled water (DI-Water) is put on the patch, and the S_{11} is found. The test results show two resonance frequencies, as seen in Figure 7(a). The first resonance is located at 2.144 GHz with a value of -11.38 dB. At the same time, the second resonance is found at 3.456 GHz with S_{11} equal to -23.57 dB. The shifting in the first resonance frequency compared with the unloaded case equals 716 MHz.

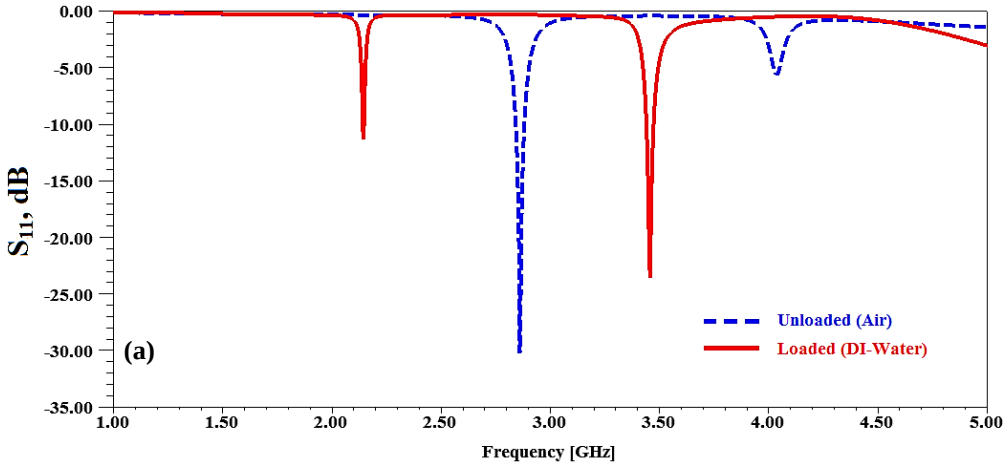

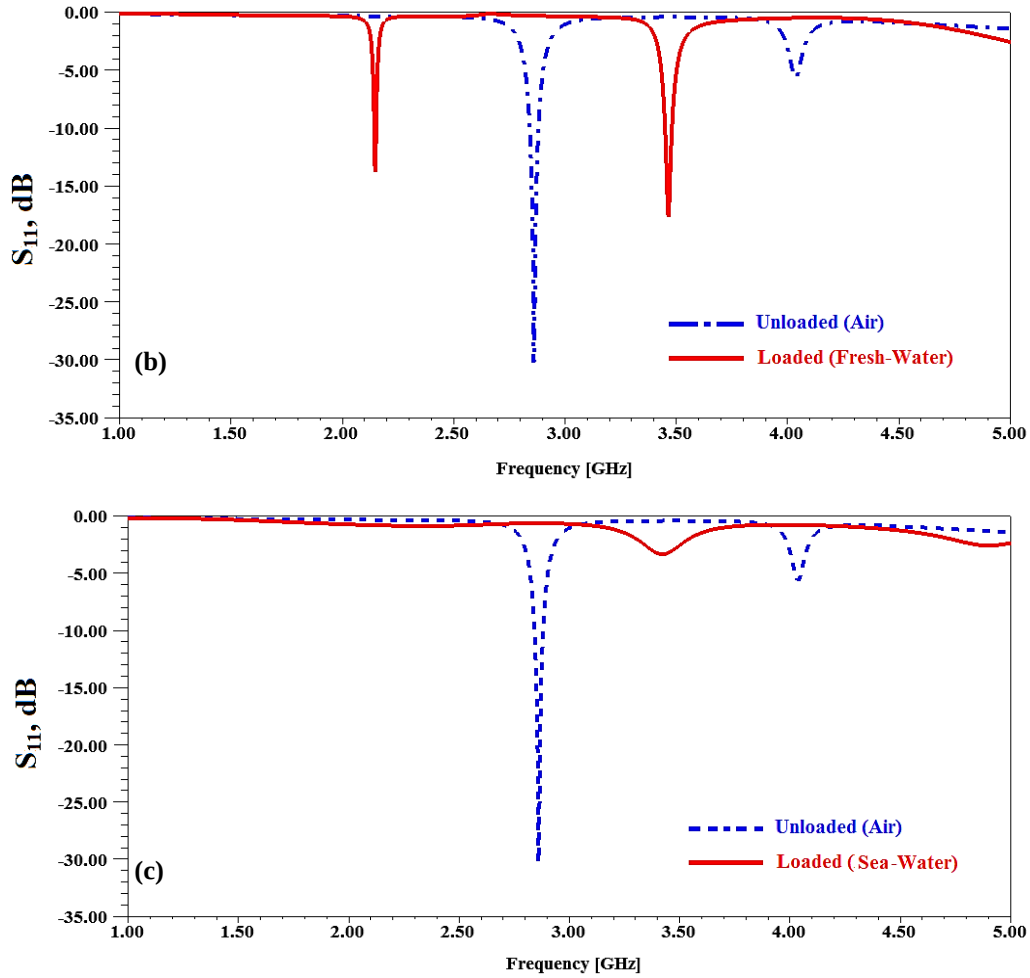

Fig. 7. S11 tested results for different water types; (a) DI-water, (b) Freshwater, and (c) Seawater

In the second test, freshwater is applied, and the S11 is measured, as seen in Fig. 7(b). The result showed two resonance frequencies at 2.148 GHz and 3.464 GHz with values equal to -13.8035 dB and -17.675 dB, respectively. By comparing the evaluated S_{11} of the unloaded case with that of freshwater, a shifting in the first resonance frequency equals 714 MHz.

Finally, seawater is applied to the patch, and the S11 is measured. The result shows a single resonance frequency at 3.41 GHz with an S11 value of -3.35 dB, as shown in Fig. 7(c). By comparing the results of seawater and unloaded conditions, a shift in the first resonance frequency is equal to 277 MHz. In Table 2, the results of all water types are compared with those from air in terms of shifting in the first resonance frequency (Δf) and S_{11} value (ΔS_{11}).

Table 2. Compares loaded and unloaded conditions regarding frequency and S11 value

Testing Liquid Type		σ(S/m)	f_r (GHz)	S_{11} (dB)	Δf (MHz)	ΔS_{11} (dB)
Unloaded-condition		0	2. 863	-30.219	-	-
Loaded	DI-Water	0.0002	2.144	-11.38	719	-18.839
	Freshwater	0.01	2.148	-13.803	715	-16.416
	Seawater	4	3.14	-3.35	0.277	-26.869

Sensitivity is defined by a ratio of the offset frequency over the offset permittivity [13]. In other words, sensitivity describes how much the output will be affected by changes in the input amount. A suitable sensor indicates that slight input changes will significantly affect the recorded output result. To obtain the sensitivity of the miniaturized inset-fed microstrip sensor, equations 4, 5, and 6 are used in reference [14-19];

$$\frac{\Delta f}{f} = \frac{|f_o - f_1|}{f_o} \quad (4)$$

$$\Delta\varepsilon = \varepsilon_o - \varepsilon_1 \quad (5)$$

$$S = \frac{\Delta f / f}{\Delta\varepsilon} \times 100\% \quad (6)$$

Where Δf is the first resonant frequency difference, f_o is the unloaded 1st resonant frequency, f_1 is the 1st resonant frequency of the loaded condition, and ε_o and ε_1 correspond to the permittivity of the reference and tested water. *S* is the sensitivity of the proposed sensor.

The proposed sensor sensitivity is evaluated and compared with the other works regarding air, seawater, and DI-water. Based on the estimated results, our proposed sensor showed high sensitivity, with values equal to 3.139 and 1.209 relative to DI-water and seawater, respectively, as shown in Table 3.

Table 3. Proposed sensor sensitivity compared with other research works for DI and seawater

Reference	f_o (GHz)	f (GHz)	$\lvert\Delta f\rvert$(GHz)	$\lvert\Delta S_{11}\rvert$ (dB)	sensitivity ($\times 10^{-3}$)
[20][1]	0.92	1	0.08	-10	1.09
[21][1]	1.18	1.52	0.34	-11	3.6
[22][1]	3.07	3.38	0.31	-	1.26
[23][1]	3.88	3.66	0.22	-5	0.72
[23][2]	3.88	3.39	0.49	-15	1.86
This work[1]	2.863	2.144	0.719	-18.839	3.139
This work[2]	2.863	3.14	0.277	-26.869	1.209

[1] References for air and DI-water, [2] References for air and seawater.

4. Conclusion

A low-cost microstrip-patch sensor antenna based on a meander-slot line was proposed in this literature for water-type identification applications. The HFSS tool was used to design and simulate the proposed sensor. The low-cost FR-4 dielectric material was used to design the sensor with dimensions equal to 60×50×1 mm^3. The meander-line slots technique produced high electric fields with significant energy by concentrating the current in a narrow area. The sensor resonated at 2.863 GHz for the unloaded condition, while it resonated at 2.144 GHz, 2.148 GHz, and 3.14 GHz for DI, fresh, and seawater in the case of the loaded state. High sensitivity values have been achieved. The sensor recorded sensitivity values of 3.14 and 1.21 for DI-water and seawater, respectively. The high sensitivity values indicate that any change in the water-type surrounding the sensing area will be translated into significant changes in the resonant frequency, as each type of water has different properties.

Acknowledgement

The authors thank the Department of Computer Engineering Techniques, Electrical Engineering Technical College, Middle Technical University, Baghdad, Iraq, for supporting this work.

References

[1] Abdelwahab, H.; Ebrahimi, A.; Tovar-Lopez, F.J.; Beziuk, G.; Ghorbani, K. Extremely Sensitive Microwave Microfluidic Dielectric Sensor Using a Transmission Line Loaded with Shunt LC Resonators. Sensors 2021, 21, 6811. https://doi.org/10.3390/s21206811.
[2] Bouchalkha A, Karli R, Alhammadi K. Reusable Sensor for Strontium Sulfate Scale Monitoring in Seawater. Materials (Basel). 2021 Feb 1;14(3):676, https://doi.org/10.3390/ma14030676.
[3] Kumari R, Patel PN, Yadav R. An ENG resonator-based microwave sensor for the characterization of aqueous glucose. J Phys D: Appl Phys. 2018; 51(7):3201-3207, DOI 10.1088/1361-6463/aaa5c5.
[4] Ebrahimi A, Withayachumnankul W, Al-Sarawi S, Abbott D. High-sensitivity metamaterial-inspired sensor for microfluidic dielectric characterization. IEEE Sens J. 2014;14(5):1345-1351, https://doi.org/10.1109/JSEN.2013.2295312.
[5] Kayal S, Shaw T, Mitra D. Design of miniaturized highly sensitive liquid sensor at microwave frequency. Int J RF Microw Comput Aided Eng. 2020;e22387. https://doi.org/10.1002/mmce.22387.
[6] D. M. Pozar, "Microstrip antennas," Proceedings of the IEEE, vol. 80, no. 1, pp. 79-91, Jan. 1992, doi: 10.1109/5.119568.
[7] J. Q. Howell, "Microstrip antennas," IEEE APS Int. Symp. Digest, pp. 177-180, 1972.
[8] R. E. Munson, "Conformal Microstrip Antennas and Microstrip Phased Arrays," IEEE Transactions on Antennas and Propagation, vol. 22, no. 1, pp. 74-78, Jan 1974.
[9] Zaid A. Abdul Hassain, Amer A. Osman, and Adham R. Azeez," First order parallel coupled BPF with wideband rejection based on SRR and CSRR," Telkomnika, Vol.17, No.6, PP. 2704-2712, December 2019, http://doi.org/10.12928/telkomnika.v17i6.10790.
[10] Zaid A. Abdul Hassain, Adham R. Azeez, Mustafa M. Ali, and Taha A. Elwi," A Modified Compact Bi-Directional UWB Tapered Slot Antenna with Double Band-Notch Characteristics," Advanced Electromagnetics, Vol. 8, No. 4, PP. 74-79, September 2019, DOI: 10.7716/aem.v8i4.1130.
[11] Zaid A. Abdul Hassain, Mustafa Mahdi Ali, and Adham R. Azeez," Single and Dual Band-Notch UWB Antenna Using SRR / CSRR Resonators, " Journal of Communications, Vol. 14, No. 6, PP. 504-510, June 2019, doi:10.12720/jcm.14.6.504-510.
[12] Ansoft's High Frequency Structure Simulator (HFSS). [Online]. Available: http://www.ansoft.com/.
[13] Abdolrazzaghi, M.; Daneshmand, M.; Iyer, A.K. Strongly enhanced sensitivity in planar microwave sensors based on metamaterial coupling. IEEE Trans. Microw. Theory Tech. 2018, 66, 1843–1855, https://doi.org/10.1109/TMTT.2018.2791942.
[14] Boybay, M.S.; Ramahi, O.M. Material characterization using complementary split-ring resonators. IEEE Trans. Instrum. Meas. 2012, 61, 3039–3046, https://doi.org/10.1109/TIM.2012.2203450.
[15] Ebrahimi, A.; Withayachumnankul, W.; Al-Sarawi, S.; Abbott, D. High-sensitivity metamaterial-inspired sensor for microfluidic dielectric characterization. IEEE Sens. J. 2014, 14, 1345–1351, https://doi.org/10.1109/JSEN.2013.2295312.
[16] Adham R. Azeez, Ahmed, S., Zalzala, A., Abdul Hassain, Z., Elwi, T.; Design of High Gain UWB Vivaldi Antenna with Dual Band-Notches Characteristics. International Journal on Engineering Applications (IREA) 2023, 11, 128-136, DOI 10.15866/irea.v11i2.22177.
[17] Yeo, J.; Lee, J.-I. High-sensitivity microwave sensor based on an interdigital-capacitor-shaped defected ground structure for permittivity characterization. Sensors 2019, 19, 498, https://doi.org/10.3390/s19030498.
[18] Salim, A.; Lim, S. Complementary split-ring resonator-loaded microfluidic ethanol chemical sensor. Sensors 2016, 16, 1802, https://doi.org/10.3390/s16111802.
[19] Yeo, J.; Lee, J.-I. Slot-loaded microstrip patch sensor antenna for high-sensitivity permittivity characterization. Electronics 2019, 8, 502, https://doi.org/10.3390/electronics8050502.
[20] Mariotti, C.; Su,W.; Cook, B.S.; Roselli, L.; Tentzeris, M.M. Development of Low Cost,Wireless, Inkjet Printed Microfluidic RF Systems

and Devices for Sensing or Tunable Electronics. IEEE Sens. J. 2015, 15, 3156–3163, https://doi.org/10.1109/JSEN.2014.2374874.

[21] Ebrahimi, A.;Withayachumnankul,W.; Al-Sarawi, S.F.; Abbott, D. Microwave microfluidic sensor for determination of glucose concentration in water. In Proceedings of the IEEE 15th Mediterranean Microwave Symposium, Lecce, Italy, 30 November–2 December 2015, https://doi.org/10.1109/MMS.2015.7375441.

[22] Jankovic, N.; Radonic, V. A Microwave Microfluidic Sensor Based on a Dual-Mode Resonator for Dual-Sensing Applications. Sensors 2017, 17, 2713, https://doi.org/10.3390/s17122713.

[23] Bouchalkha, A., Karli, R., and Alhammadi, K," Reusable Sensor for Strontium Sulfate Scale Monitoring in Seawater," Materials 2021, 14, 676. https://doi.org/10.3390/ma14030676.